JVST A
Journal of Vacuum Science & Technology A

ARTICLE

avs.scitation.org/journal/jva

Thermal etching of AlF_3 and thermal atomic layer etching of Al_2O_3

Cite as: J. Vac. Sci. Technol. A 38, 022603 (2020); doi: 10.1116/1.5135911
Submitted: 8 November 2019 · Accepted: 30 December 2019 ·
Published Online: 14 January 2020

Andreas Fischer,[1,a)] Aaron Routzahn,[1] Younghee Lee,[1] Thorsten Lill,[1] and Steven M. George[2]

AFFILIATIONS

[1]Lam Research Corporation, 4400 Cushing Parkway, Fremont, California 94538
[2]Department of Chemistry, University of Colorado at Boulder, Boulder, Colorado 80309

Note: This paper is part of the Special Topic Collection Commemorating the Career of John Coburn.
[a)]**Electronic mail:** andreas.fischer@lamresearch.com

ABSTRACT

Thermal etching of AlF_3 with dimethyl-aluminum chloride (DMAC) and thermal isotropic atomic layer etching (ALE) of Al_2O_3 with alternating anhydrous hydrogen fluoride (HF) and DMAC steps were studied. DMAC vapor etches AlF_3 spontaneously at substrate temperatures above 180 °C. The thermal etching reaction of AlF_3 with DMAC exhibited no self-limitation and showed a linear dependence on DMAC pressure. The authors determined an activation energy of 1.2 eV for this reaction. When Al_2O_3 is fluorinated, DMAC removes the fluorinated layer partially. The etch amount per cycle (EPC) in thermal isotropic ALE of Al_2O_3 with HF/DMAC is primarily determined by the fluorination step placing significant importance on its design. Fluorination with HF gas was found to be more effective and repeatable than with NF_3. Plasma fluorination is faster and provides higher EPC, but the selectivity to Si_3N_4 or SiO_2 mask materials is compromised. For pressures between 10 and 110 mTorr and a substrate temperature of 250 °C, thermal ALE of Al_2O_3 with HF/DMAC was found to have a very high selectivity to SiO_2 and amorphous silicon. HfO_2, however, etched with similar EPC as Al_2O_3.

I. INTRODUCTION

In the mid-1970s, John Coburn began the study of reactive ion etching (RIE) together with his co-worker Harold Winters. The focus of their work was on the surface science aspects of the involved mechanisms.[1] In 1979, they published their seminal paper describing the synergy between ions and neutrals in a beam experiment with XeF_2 neutrals and argon ions.[2] The combination of the two beams produced a large enhancement in the material removal rate due to the mechanism of RIE. In a modern-day interpretation of their result, one could say that had they alternated between the XeF_2 neutral and argon ion beams, they would have produced the first directional atomic layer etching (ALE) process. Winters and Coburn described the etching process as a sequence of five steps: physisorption, dissociative chemisorption, chemical reaction with the surface, desorption of the reaction product, and removal of nonreactive residues if they exist.[2,3] The last two steps are accomplished by ion bombardment in RIE and in directional ALE.

In this paper, we report on using thermal energy and a ligand exchange reaction instead of ion bombardment to stimulate desorption. ALE processes that utilize radicals and neutrals in self-limited modification and removal steps are called thermal isotropic ALE.[4] Thermal isotropic ALE has recently garnered much attention by the ALD and etching communities. It was first reported for etching of Al_2O_3 by exposure to alternating hydrogen fluoride (HF) and tin-acetylacetonate [$Sn(acac)_2$] vapor.[5] At least four classes of thermal isotropic ALE are known to date: ligand exchange ALE,[5] conversion ALE,[6] oxidation/fluorination ALE,[7] and chelation/condensation ALE.[8,9] In this work, we studied thermal isotropic ALE using a ligand exchange reaction. The Al_2O_3 surface is fluorinated in a first step and removed with dimethyl-aluminum chloride (DMAC) in a second step. This reaction as well as the related Al_2O_3 ALE with HF/trimethylaluminum (TMA) were reported previously.[10]

Thermal ALEs of Al_2O_3 with HF/$Sn(acac)_2$ and HF/TMA are considered archetypical systems for thermal isotropic ALE. For both reactions, the etch amount per cycle (EPC) increases with the temperature, but the underlying mechanisms appear to be different. Lee *et al.* found that for HF/$Sn(acac)_2$, acetylacetonate (acac) containing compounds such as SnF(acac) remain at the surface.[11] The Al_2O_3 EPC is inversely dependent on the coverage with acetylacetonate surface species, which was found to be lower at higher temperatures.

This behavior suggested that acetylacetonate surface species may have a site-blocking effect.[11] The depth of fluorination can be deeper than the EPC and the latter is determined by the site-blocking effect of acac containing compounds. These compounds must be removed by HF in the subsequent surface modification step of the ALE cycle. $Sn(acac)_2$ will not etch AlF_3 in a continuous process.[12]

TMA removes AlF_3 without site blocking. Cano *et al.* reported proportionality between the Al_2O_3 EPC and the aluminum fluoride layer thickness for thermal isotropic ALE with HF/TMA.[13] The thickness of the fluorinated layer was measured with XPS and modeled as Al_2OF_4 or a combination of AlF_3 and AlOF. The fluorinated layer thickness was found to be roughly two times the EPC, the latter increased with temperature and HF pressure. This mechanism for the fluorination of Al_2O_3 is similar to the mechanism for silicon oxidation.[13,14] The fluorination step is critical for Al_2O_3 ALE with TMA/HF because it determines the EPC. The TMA removal step is essentially a thermal etching process of AlF_3. To what degree TMA etches incompletely fluorinated aluminum AlO_xF_y is not known.

In this paper, we explore the relationship of thermal etching of fully fluorinated AlF_3 with DMAC as well as thermal ALE of Al_2O_3 with NF_3/DMAC or HF/DMAC.

II. EXPERIMENT

The experiments were conducted in a modified RIE chamber for 300 mm wafers as shown in Fig. 1. The wafer was held by an electrostatic chuck (ESC), which heated the wafer to temperatures between 150 and 280 °C. The heat was transferred via helium gas between the ESC and wafer backside surfaces allowing adequate wafer heating even at process pressures in the millitorr range. The chamber is equipped with a turbomolecular pump capable to maintain pressures between 1 and 500 mTorr. DMAC was converted from liquid to gas in a vaporizer and drawn by the process chamber vacuum to the substrate. HF and other gases were delivered from a gas cabinet. All gases were injected through a gas nozzle above the center of the wafer. Flows were between 50 and 500 SCCM for DMAC vapor and all process gases. Plasma was generated with a transformer coupled plasma source with an excitation frequency of 13 MHz,[15] resulting in ion energies in the range between 10 and 20 eV. The gap between wafer and the top window of the reactor was 15 cm. While such a large gap required several seconds long pump steps to ensure minimal intermixing of HF and DMAC in the gas volume above the wafer (optimal pump step times of 30 s were determined experimentally by maximizing EPC with all other process parameters kept constant), it allowed us to utilize a plasma source that is fully optimized for ion flux uniformity and ion energy. The reactor walls were covered with Y_2O_3; the exact details of the coating process and thickness are proprietary to the Lam Research Corporation.

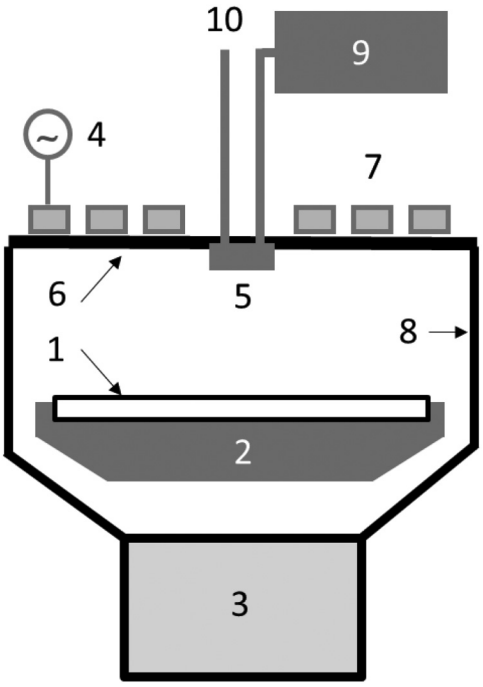

FIG. 1. Experimental setup: (1) 300 mm wafer, (2) electrostatic chuck, (3) turbo pump, (4) source RF power, (5) gas injection, (6) dielectric window, (7) inductive antenna, (8) chamber walls, (9) vaporizer, and (10) gas line from the gas box.

Some early experiments were conducted in a miniaturized version of this chamber for processing of 100 mm wafers and coupons. There, all reactor walls were stainless steel and the top window was made of yttria-coated alumina. The samples were placed on a grounded pedestal without ESC.

We used 2×2 in. coupons that were gallium-bonded to 300 mm bare silicon carrier wafers with either 24 nm thick AlF_3 or 28 nm thick Al_2O_3 deposited by ALD on top of SiO_2. In addition, patterned Al_2O_3 samples with an Si_3N_4 mask featuring 60 nm wide holes were tested.

A Thermo Fisher Scientific Theta 300 standalone XPS tool with a monochromatic Al k_α x-ray source at 1486.7 eV was utilized to characterize the surface composition. There was a queue time in air of about 30 min between sample processing and XPS measurements. Film thicknesses were measured with spectral ellipsometry and SEM cross sections.

III. RESULTS AND DISCUSSION

A. Thermal etching of AlF_3

At a pressure of 30 mTorr and a wafer temperature of 250 °C, DMAC etched AlF_3 spontaneously as shown in Fig. 2. The gas was delivered in time increments of 30 s. The etched amount of AlF_3 is a linear function of time indicating that there is no self-limitation of the etch due to an accumulation of reaction products at the surface or other impeding processes. The original AlF_3/silicon interface was reached after nearly 50 DMAC steps of 30 s each, resulting in etch stop due to the complete removal of AlF_3. We determined an etch rate of 1.04 nm/min for AlF_3. Figure 3 depicts the pressure dependence of the etching rate of this material. We found 1.50 and 2.23 nm/min at 60 and 100 mTorr, respectively. A linear trendline fits the data that indicate that the reaction is a first order surface reaction in the explored pressure range. A linear

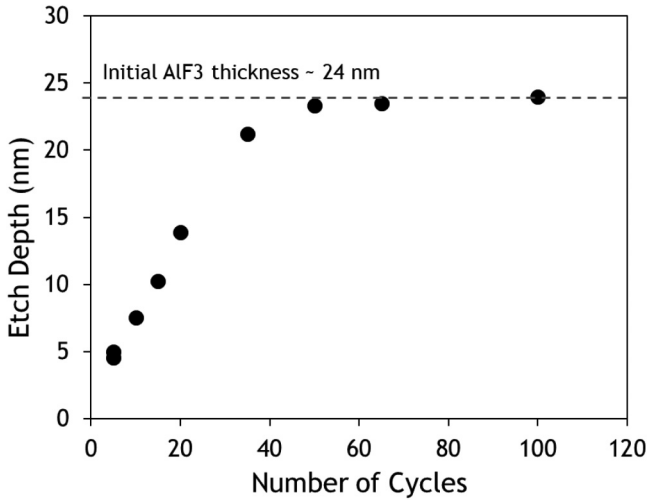

FIG. 2. Thermal etching of AlF_3 with DMAC: etched amount vs number of DMAC cycles where each cycle is 30 s long.

fit also suggests that the DMAC surface coverage does not change significantly in this pressure region.

The surface reaction is strongly temperature dependent. Below 180 °C, we observed no etching but an increase in film thickness as measured by spectral ellipsometry. The composition of this low-temperature film was not analyzed. This film may result from the formation of mixed halide complexes between DMAC and AlF_3. Above 180 °C, etching occurred with an exponential rate increase versus temperature (see Fig. 4). An activation energy of 1.2 eV can be calculated from the three measured etching rates above 180 °C using the Arrhenius approach. The corresponding Arrhenius plot is shown in Fig. 5.

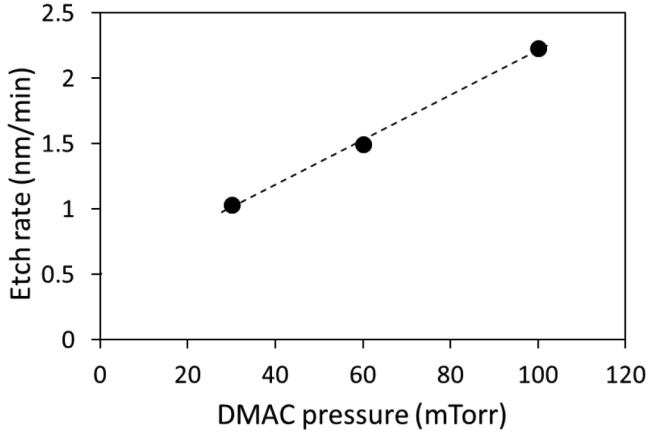

FIG. 3. Thermal etching of AlF_3 with DMAC: etching rate as a function of pressure.

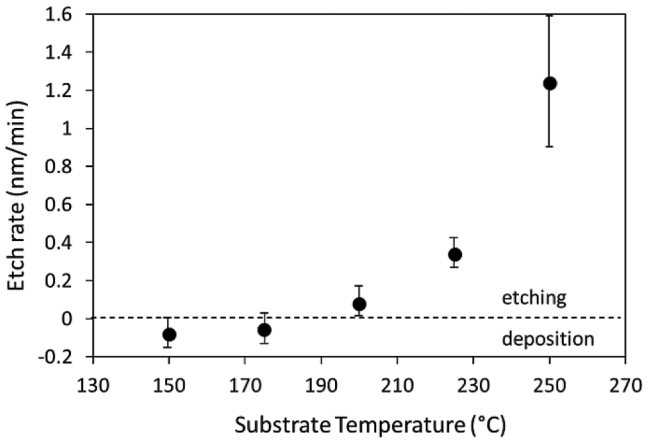

FIG. 4. Thermal etching of AlF_3 with DMAC: etching rate as a function of wafer temperature. The large error bar at 250 °C likely stems from repeatability issues in heat transfer between the carrier wafer and the AlF_3 coupon.

B. Fluorination of Al_2O_3

Thermal etching can be used to design thermal isotropic ALE processes if two conditions are met. The removal precursor must etch the modified material but not the original one, and a thermal reaction must exist, which converts the surface from the original to the modified material in a self-limited regime. DMAC has been applied in the removal step of fluorinated Al_2O_3 previously.[10,16] Because DMAC etches AlF_3 thermally, the EPC of the reaction is determined by the depth of fluorination. The fluorination step is therefore critically important for this reaction.

We explored various fluorination methods using NF_3 and anhydrous HF via thermal fluorination and with plasma. Figure 6

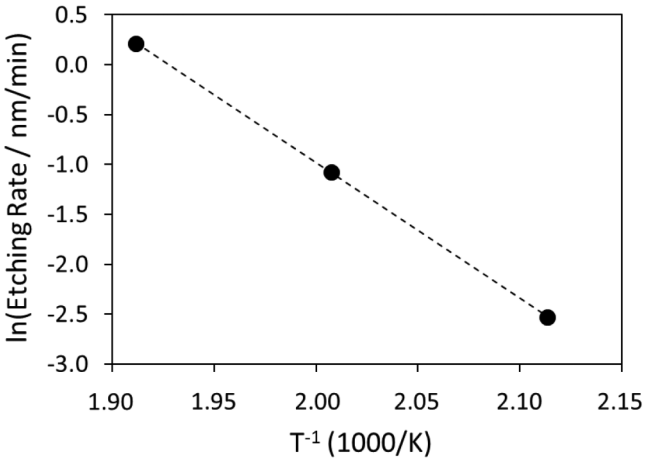

FIG. 5. Arrhenius plot for thermal etching of AlF_3 with DMAC. Vertical axis shows the natural logarithm of the etch rate measured in nanometers per minute.

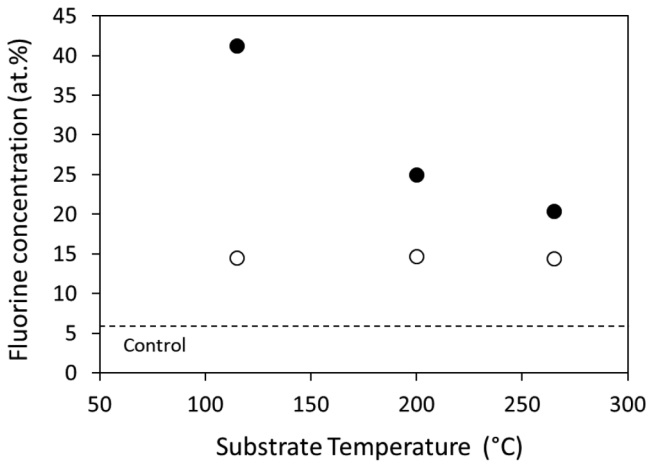

FIG. 6. Fluorine concentration at the surface of Al_2O_3 after fluorination with NF_3 gas and plasma as a function of temperature.

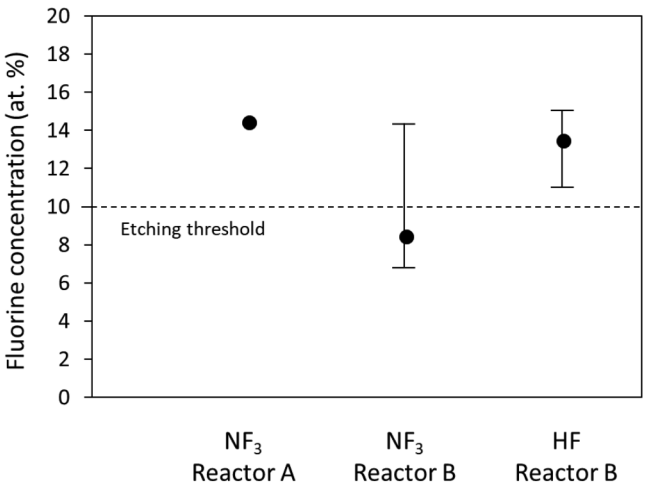

FIG. 7. Fluorine concentration at the surface of Al_2O_3 after fluorination with NF_3 and anhydrous HF gas for two different reactors. A: Small scale reactor with stainless steel walls; B: 300 mm reactor with Y_2O_3 covered walls.

compares the fluorination of Al_2O_3 with NF_3 gas and NF_3 inductively coupled plasma. The experiments were conducted in a stainless steel reactor. The pressure was 100 mTorr and the source power was 400 W in the case of plasma fluorination. For thermal fluorination, the surface fluorine concentration was 15 at. % and showed no detectable temperature dependence. As the attenuation length for photoelectrons stemming from fluorine atoms is four times larger than the penetration depth of fluorine into Al_2O_3,[17] the fluorine signal can be used as a good approximation for the actual fluorine concentration.

Plasma fluorination using NF_3 achieved fluorine concentrations of up to 41 at. % at 120 °C. The concentration dropped to 20% at 265 °C approaching the value of thermal fluorination. Unlike in a thermal process, plasma can deliver fluorine in ion and radical form to the substrate surface thereby greatly increasing the reactivity with the surface. As a result, a far greater fluorine amount is adsorbed initially than in a purely thermal process. Higher substrate temperature, however, increases the surface desorption rate of physically bonded fluorine in agreement with the measured concentration drop reported above. This temperature behavior of plasma fluorination is different from the previously reported thermal fluorination where diffusion of fluorine into the subsurface lattice was found to accelerate with the temperature.[13] While plasma appears promising for deeper fluorination and to achieve larger EPC, we find that using plasma in the fluorination step severely compromised selectivity to mask materials such as Si_3N_4 or SiO_2.

Thermal fluorination with NF_3 was not effective in the large-scale reactor featuring alumina and yttria walls. The fluorine surface concentrations were lower and exhibited a large sensitivity to various wall treatments with plasma and were not repeatable as indicated by the large error bar in Fig. 7. The fluorine concentration was, on average, below 10% resulting in negligible EPCs when DMAC was applied. We attribute the difference in thermal fluorination with NF_3 to the difference in reactor wall materials (stainless steel versus Y_2O_3). Sensitivity of the ALE process with respect to the surrounding surfaces was previously reported for Al_2O_3 ALE with HF/TMA.[18] Hennessy *et al.* did not partition whether the sensitivity to LiF near the wafer was caused by the HF or the TMA step.[18] Nevertheless, there is emerging evidence that reactor wall materials must be taken into consideration when comparing EPC's of the same thermal ALE chemistry.

Fluorination with HF yielded fluorine surface concentrations well above the etching threshold, and the results were repeatable. A close analysis of the Al 2p XPS peak at 75.5 eV did confirm the

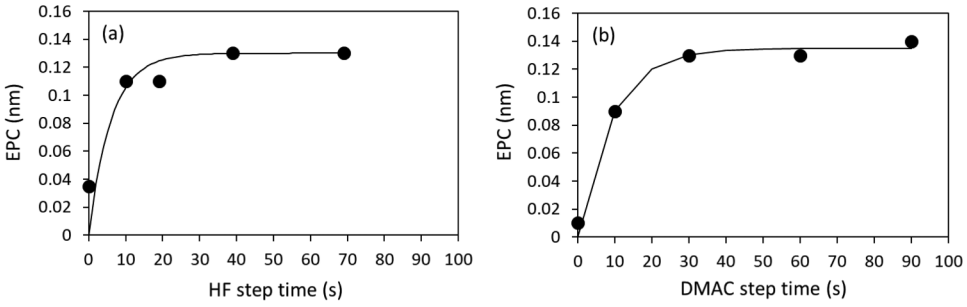

FIG. 8. Saturation curves for thermal ALE of Al_2O_3 with HF/DMAC at 30 mTorr and 250 °C with DMAC step time kept constant at 30 s (a) and HF step time kept constant at 30 s (b).

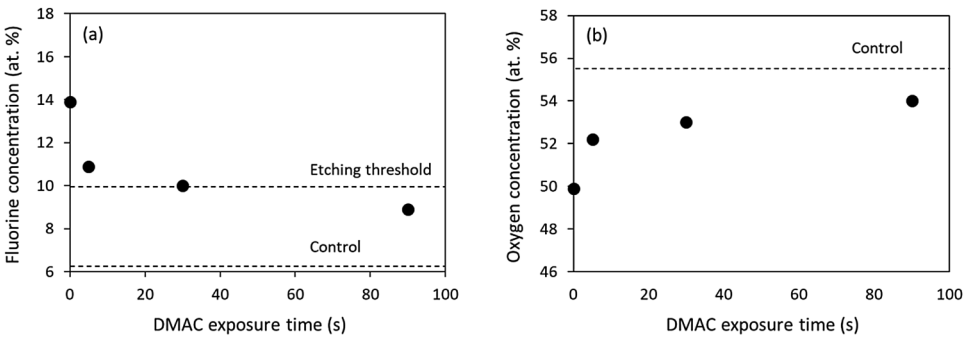

FIG. 9. Fluorine (a) and oxygen (b) concentrations at an Al_2O_3 surface after HF exposure and subsequent DMAC exposure as a function of DMAC exposure time.

presence of aluminum oxyfluoride but displayed no discernable evidence that the formation of AlF_3 had taken place. This result is in agreement with Cano *et al.*[13] Both XPS measurements were conducted with air exposure between fluorination and analysis. Therefore, we cannot completely exclude the existence of incipient AlF_3, which is converted back to an oxyfluoride during air exposure (prior to XPS).

C. Thermal ALE of Al_2O_3

Thermal ALE of Al_2O_3 is achieved by combining the HF fluorination step with DMAC removal of AlF_3. The condition of apparent self-limitation of both steps is met after about 30 s of gas flow (see Fig. 8) at a temperature of 250 °C with the entire process being run at a constant pressure of 30 mTorr. The resulting EPC was 0.14 nm. Previously, EPC values of 0.032 nm have been reported for ALD deposited Al_2O_3 at the same temperature.[10] Differences between the two experiments include the Al_2O_3 film preparation, the fluorination precursor (HF-pyridine versus anhydrous HF), pressure (partial versus absolute pressure) and reactor wall materials (alumina-coated stainless steel versus yttria-coated aluminum).

Figure 9 shows the evolution of the fluorine surface concentration during exposure to DMAC. The fluorine surface concentration dropped from 14% to 9% after 90 s treatment with DMAC at 30 mTorr. The control value of a sample, which was not treated with HF, was 6%. At the same time, the oxygen concentration increased from 50% to 54%. These findings are consistent with a gradual re-establishing of the original Al_2O_3 surface under DMAC exposure by removing the fluorinated top layer.

As AlF_3 was consumed entirely by thermal etching with DMAC (see Fig. 2), we conclude that the prevalent material on the surface after thermal fluorination must be an aluminum oxyfluoride and cannot be AlF_3. It is possible that residual fluorine is bonded to aluminum, which is also bonded to oxygen, that fluorine is not bonded to aluminum at all (F_2 or HF), or that it is bonded to fully fluorinated aluminum, which is surrounded by aluminum oxide compounds and not accessible to DMAC.

Figure 10 shows the fluorine surface concentration immediately after HF treatment as a function of temperature. We noticed that fluorine concentration with HF was generally higher compared to the thermal values achieved with NF_3 likely due to the higher reactivity of HF. However, like in the plasma case described above and in Fig. 6, the concentrations dropped with increasing temperature (unlike in the thermal NF_3 case), approaching 15%, again due to the increased surface desorption rates at a higher temperature.

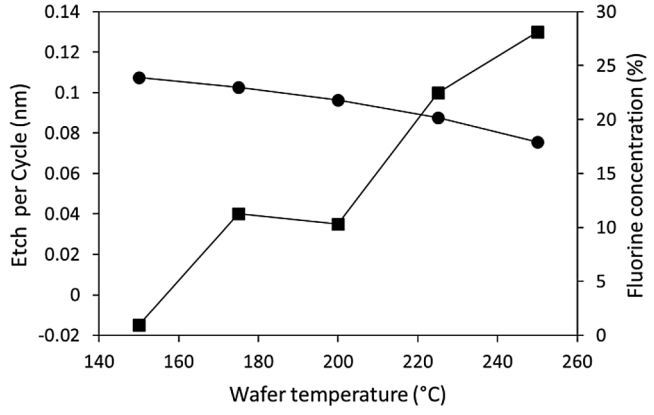

FIG. 10. Fluorine concentration after HF exposure and EPC of Al_2O_3 ALE with HF/DMAC as a function of wafer temperature.

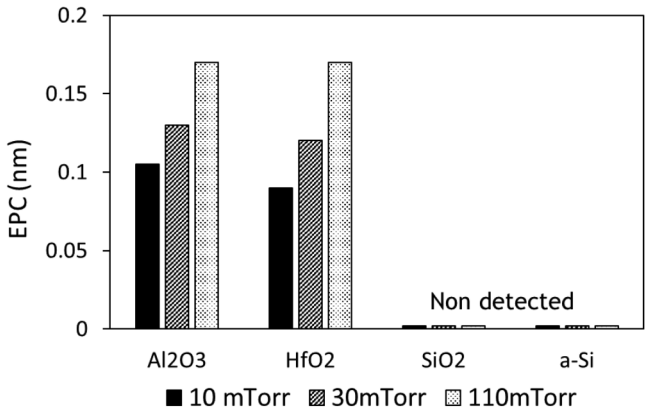

FIG. 11. EPC for HF/DMAC ALE for Al_2O_3, HfO_2, SiO_2, and amorphous silicon at 250 °C as function of pressure.

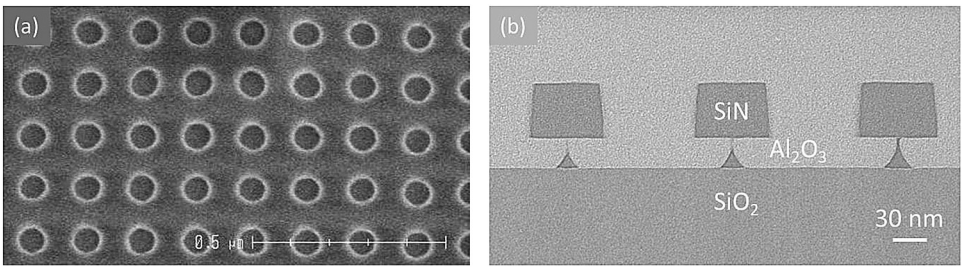

FIG. 12. Top-down SEM of a sample before Si_3N_4 mask open and resist strip (a) and cross section of the same sample after 1000 ALE cycles (b).

A nonzero EPC was observed above 170 °C, which is very similar to the etching threshold observed for thermal etching of AlF_3 with DMAC. Hence, the lower limit of the ALE window is determined by the reactivity of DMAC. EPC increases strongly with the temperature despite a decreasing fluorine surface concentration after the HF step. We attribute the increase in EPC with temperature to an increasing reactivity of DMAC with aluminum oxyfluoride. This response to temperature should be exponential as with pure AlF_3 shown in Fig. 4 and should compensate for the lowered fluorine concentration at higher temperatures.

Thermal ALE with HF/DMAC etched Al_2O_3 and HfO_2 with similar EPCs but no etching of SiO_2 nor amorphous silicon was found for pressures between 10 and 110 mTorr as shown in Fig. 11. The pressure was the same in both steps. DuMont *et al.* reported etching of SiO_2 with HF/TMA at 300 °C via a conversion reaction for pressures above 100 mTorr and particularly above 1 Torr.[6] We did not observe this mechanism for HF/DMAC for pressures of up to 110 mTorr. The EPCs for Al_2O_3 and HfO_2 increased by over 50% from 10 to 110 mTorr. We cannot discern from our data whether the HF or the DMAC step caused this increase because the pressure in both steps was increased. Cano *et al.* reported an increase in fluoride thickness with pressure with a steep increase below 1 Torr and a flattening curve above 4 Torr.[13]

Etch selectivities do not always transfer from tests with individual coupons to wafers where all materials are colocated. This is a known etching effect called microloading.[19] Based on the sensitivity of the process to the reactor walls, we must assume that it also exists in thermal isotropic ALE. To test this, 26 nm Al_2O_3 was deposited on SiO_2 and patterned with 45 nm Si_3N_4. The hole openings were 60 nm. The samples were etched in a viscous flow reactor at the University of Colorado[20] for 500 cycles at 300 °C at 25 mTorr partial pressure. The etch uniformity from the front to the back of the reactor is estimated to be better than 10% (min-max) based on ALD results. We could not detect any Si_3N_4 or SiO_2 loss in the cross-sectional electron micrograph shown in Fig. 12. The isotropic nature of the process is clearly visible from the lateral etching. A more detailed analysis of the vertical and normal etching amount will be the subject of future studies.

IV. CONCLUSIONS

DMAC gas etches AlF_3 in a continuous process at temperatures above 180 °C with an activation energy of 1.2 eV. We used this reaction to realize a thermal ALE process where Al_2O_3 is converted to aluminum oxyfluoride and potentially AlF_3 via exposure to fluorine containing gases and subsequently removed by DMAC. We found fluorination with HF more repeatable and less sensitive to chamber wall materials compared to NF_3. Etching was detected for the HF/DMAC process for temperatures above 170 °C and increases with temperature despite lower fluorine concentration. We attribute this behavior to an increased reactivity of DMAC with aluminum oxyfluoride.

Very high selectivity to SiO_2 and Si_3N_4 was measured both on blanket and patterned wafers. HfO_2, however, etched with a similar EPC as Al_2O_3. Re-entrant profiles demonstrate the isotropic nature of this thermal ALE process.

Over 40 years after John Coburn pioneered RIE, new and useful etching technologies are still being discovered. Thermal isotropic ALE leverages the body of knowledge of the etching and ALD communities. John Coburn's emphasis on etching fundamentals is an inspiration for new generations of researchers and practitioners of this essential integrated circuit processing technology.

ACKNOWLEDGMENTS

The authors would like to thank Emir Gurer and Zinki Garg for the XPS measurements and analysis of the data, Paul Lemaire for preparing the AlF_3 films, and Richard Janek for the mask open processing.

REFERENCES

[1]J. W. Coburn, Appl. Phys. A **59**, 451 (1994).
[2]J. W. Coburn and H. F. Winters, J. Appl. Phys. **50**, 3189 (1979).
[3]H. F. Winters, J. Appl. Phys. **49**, 5165 (1978).
[4]K. J. Kanarik, T. Lill, E. A. Hudson, S. Sriraman, S. Tan, J. Marks, V. Vahedi, and R. A. Gottscho, J. Vac. Sci. Technol. A **33**, 020802 (2015).
[5]Y. Lee and S. M. George, ACS Nano **9**, 2061 (2015).
[6]J. W. DuMont, A. E. Marquardt, A. M. Cano, and S. M. George, ACS Appl. Mater. Interfaces **9**, 10296 (2017).
[7]Y. Lee and S. M. George, Chem. Mater. **29**, 8202 (2017).
[8]J. K. C. Chen, N. D. Altieri, T. Kim, E. Chen, T. Lill, M. Shen, and J. P. Chang, J. Vac. Sci. Technol. A **35**, 05C305 (2017).
[9]E. Mohimi, X. I. Chu, B. B. Trinh, S. Babar, G. S. Girolami, and J. R. Abelson, ECS J. Solid State Sci. Technol. **7**, 491 (2018).
[10]Y. Lee, C. Huffman, and S. M. George, Chem. Mater. **28**, 7657 (2016).
[11]Y. Lee, J. W. DuMont, and S. M. George, Chem. Mater. **27**, 3648 (2015).
[12]Y. Lee, J. W. DuMont, and S. M. George, J. Phys. Chem. C **119**, 25385 (2015).
[13]A. M. Cano, A. E. Marquardt, J. W. DuMont, and S. M. George, J. Phys. Chem. C **123**, 10346 (2019).
[14]B. E. Deal and A. S. Grove, J. Appl. Phys. **36**, 3770 (1965).

[15]J. B. Carter, J. P. Holland, E. Peltzer, B. Richardson, E. Bogle, H. T. Nguyen, Y. Melaku, D. Gates, and M. Ben-Dor, J. Vac. Sci. Technol. A **11**, 1301 (1993).
[16]Y. Lee and S. M. George, J. Phys. Chem. C **123**, 18455 (2019).
[17]A. Fischer, R. Janek, J. Boniface, T. Lill, K. J. Kanarik, Y. Pan, V. Vahedi, and R. A. Gottscho, Proc. SPIE **10149**, 101490H (2017).
[18]J. Hennessy, C. S. Moore, K. Balasubramanian, A. D. Jewell, K. France, and S. Nikzad, J. Vac. Sci. Technol. A **35**, 041512 (2017).
[19]C. Hedlund, H.-O. Blom, and S. Berg, J. Vac. Sci. Technol. A **12**, 1962 (1994).
[20]J. W. Elam, M. D. Groner, and S. M. George, Rev. Sci. Instrum. **73**, 2981 (2002).